

Measuring Terrestrial Interference Properties at DSS-13 at 32 GHz

Ted Peng,* Christian Ho,* Stephen Slobin,† Dennis Lee,* and Peter Kinman‡

ABSTRACT. — The Spectrum Engineering Group conducted a series of terrestrial interference tests at Goldstone, California, on October 23–25, 2009, using Deep Space Station (DSS)–13 to receive at 32 GHz. The role of interfering emitter was played by a 1-W transmitter and a 1-m dish antenna. Three locations were used for the emitter: 2.1 km distant from DSS-13 with line of sight (LOS), 3.8 km distant without LOS, and 32.4 km distant without LOS. At the two latter locations, the LOS was blocked by hills near DSS-13. At each location, the emitter antenna was first pointed toward DSS-13 and the power received at DSS-13 was measured. (For the locations without LOS, the emitter antenna was pointed along the great circle path toward DSS-13.) Then the emitter antenna was pointed away from DSS-13 along an azimuthal direction (that is, horizontally) in order to measure the resulting decrease in received power. Measured data indicated that when the emitter antenna was pointed toward DSS-13, the measured received power agreed to within about 3 dB of the calculated received power. The calculated received power was based on the propagation loss models of the International Telecommunication Union (ITU). More importantly, it was found that when the emitter antenna was pointed away from DSS-13, the received power decreased more slowly with azimuthal angular offset for the two locations with no LOS, relative to the LOS case. The lesson from this is that for Deep Space Network (DSN) antennas to be adequately protected from trans-horizon interferers, interferer antennas should be pointed away from the great circle path to the DSS by a substantial offset.

I. Introduction

Deployment of commercial data communication terminals in the band 37.0 to 38.0 GHz is expected as part of the high-density applications in the fixed service (HDFS) allocation of the International Telecommunication Union (ITU). Analytical studies have shown that 37-GHz HDFS emitters in the vicinity of deep-space stations (DSSs) must have limitations if they are not to violate the Space Research Service interference protection criteria [1]. These limitations are necessary even considering the site shielding afforded the DSS by nearby hills. These considerations apply to the DSSs in Goldstone (California), Robledo (Spain), and Tidbinbilla (Australia).

* Communications Architectures and Research Section.

† Communications Ground Systems Section.

‡ California State University, Fresno.

The necessary limitations can be managed by partitioning the area surrounding each DSS into zones and estimating the contribution of each zone's emitters to the interference received at the DSS [1]. The contribution from any one zone is found from an aggregate equivalent isotropically radiated power (EIRP) for the zone and in the direction of maximum power delivery to the DSS. This aggregate EIRP depends on the number of emitters in the zone, their transmit powers, and the directions with which their antennas point. When calculations of this type are done, it is sometimes found that one or a small number of emitters dominates the aggregate EIRP when the antennas of those emitters point low to the horizon and near the great circle path toward the DSS. For those offending emitters, it is important to have a mitigation study. A mitigation study would suggest a minimum offset angle by which an emitter antenna should point away from the DSS. If an emitter has a line of sight (LOS) to the DSS, the reduction of received power caused by the offset angle is easily estimated using the gain pattern of the emitter antenna. However, when there is no LOS between emitter and DSS, it is much more difficult to model the power reduction as a function of offset angle.

The ITU Radiocommunication sector (ITU-R) recommends that received power P_r (dBm) be estimated as

$$P_r = P_t + G_t - L_b + G_r \quad (1)$$

where P_t is the emitter (transmit) power (dBm), G_t and G_r (dBi) are the antenna gains, and L_b (dB) is the basic transmission loss (propagation loss) [2]. When there is no LOS, G_t is the gain of the emitter antenna in a direction defined by the azimuth of the great circle path toward the DSS and an elevation equal to the horizon elevation angle along that azimuth. The horizon elevation angle for any given azimuth of the antenna is the minimum elevation angle corresponding to a straight-line path to the top of the terrain feature defining the horizon. The propagation loss L_b is obtained from models that use the terrain profile (terrain height as a function of distance) for the path segment separating the emitter and the DSS. This procedure for estimating received power is convenient because the only terrain information it requires is the two-dimensional terrain profile. Equation (1) can also be used to estimate the received power coming from a zone of emitters if $P_t + G_t$ is interpreted as the aggregate EIRP of the zone (and if a common L_b and a common G_r can be assumed) [1]. The use of Equation (1) with a two-dimensional terrain profile is convenient but does not provide the best accuracy in all cases. The basis for that model is the assumption that the dominant path for the delivery of interference power lies within the vertical plane defined by the great circle path from the emitter to the DSS. This assumption is generally invalid when there is no LOS. In the case where a trans-horizon emitter antenna has a small offset angle from the azimuth of the great circle path toward the DSS and an elevation angle approximately equal to the horizon elevation angle, the dominant path for the delivery of interference power may well lie in the (nonvertical) plane defined by the emitter, the boresight of the emitter antenna, and the DSS. Although the angle of diffraction (or troposcattering) is somewhat larger for this path, causing larger losses, the effect may be more than compensated by the large boresight gain of the emitter antenna.

Figure 1 is a simple illustration of the diffraction on a ridgeline and two possible paths. The path (V) in the vertical plane is the shortest path with the smallest angle of diffraction; however, the boresight of the emitter antenna does not lie along this path. The path (B) following the boresight experiences a slightly longer path and a somewhat larger angle of diffraction.

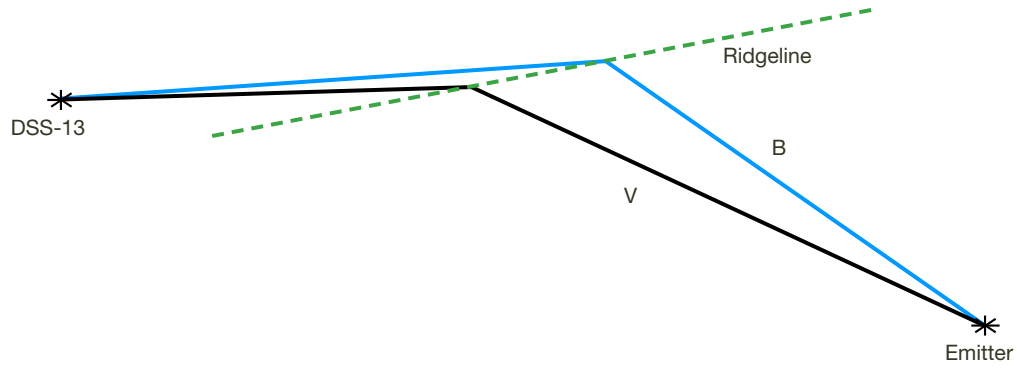


Figure 1. Simple illustration of trans-horizon paths: V = vertical-plane path; B = boresight path.

The series of measurements reported here was motivated by a need to understand the relationship between the offset angle of an emitter antenna and the power delivered to a DSS when no LOS exists. A definitive model for this relationship is not possible at this time. However, measurements reported here provide the first step in understanding this relationship for some example geometries. If needed, the method developed here can be applied to any DSS in a more comprehensive manner.

The measurements were made at DSS-13 using a frequency of 32 GHz. At present, no DSS receives at 37 GHz. In the future, the 34-m antennas of the DSN are likely to be equipped for reception at 37 GHz. Several of the 34-m DSSs, including DSS-13, are equipped for reception at 32 GHz. DSS-13 was selected because it is the research station; the other 34-m antennas have busy operational schedules. It should be noted that the 32-GHz measurements provide only a reference point and an approximation to the true characteristics at 37 GHz.

II. Emitter and Emitter Locations

A transmitter with a maximum transmit power of 1 W and a 1-m portable, offset-fed, dish antenna were selected to play the role of HDFS emitter. The primary reflector of the antenna is an ellipse with major axis 1.0 m and minor axis 0.9 m.

In assessing candidate sites for the emitter, the terrain was taken into account. It was necessary that the emitter would deliver a measurable power to DSS-13 with that station pointing low to the horizon and along the azimuth toward the emitter. For each candidate site, the propagation loss was estimated using the models of ITU-R P.452 [2] and the terrain profile along the great circle path between the candidate site and DSS-13. Maps of propagation

loss, calculated using the ITU-R models, for the area surrounding the Goldstone complex have been published previously [3].

Three sites were selected. The locations are specified relative to DSS-13 in Table 1. A map showing these sites appears in Figure 2. Sites 2 and 3 lie beyond the horizon of DSS-13.

Table 1. Location of emitter as viewed from DSS-13.

Site	Distance	LOS?	Azimuth Angle at DSS-13	Elevation Angle at DSS-13
1	2.1 km	yes	55.0 deg	-3.1 deg
2	3.8 km	no	110.5 deg	-1.4 deg
3	32.4 km	no	164.2 deg	-1.0 deg

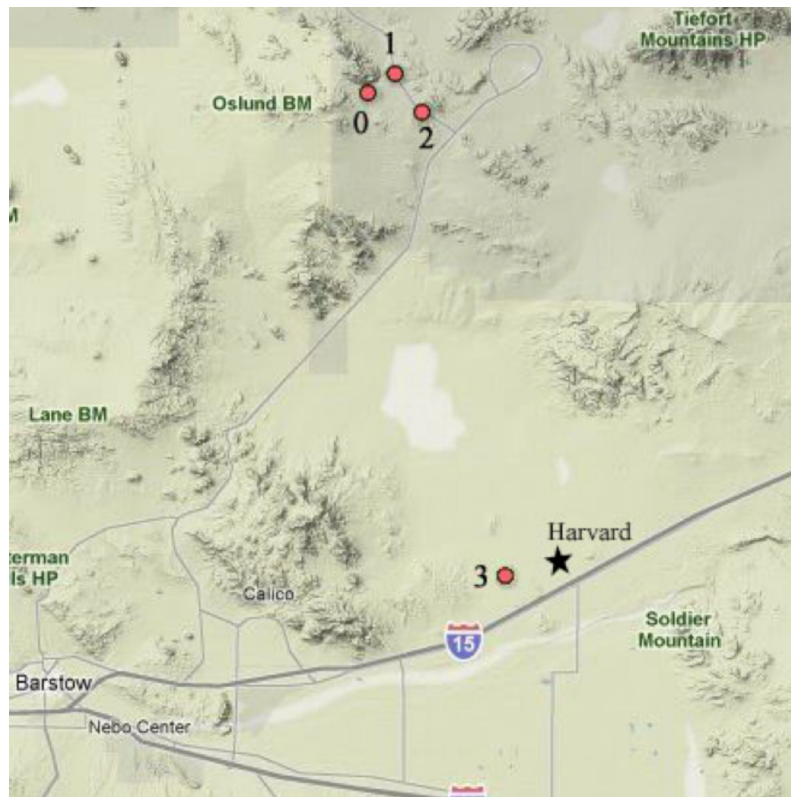


**Figure 2. Locations: 0 = DSS-13; 1 = Site 1; 2 = Site 2; 3 = Site 3.
Image: Google Maps™ mapping service.**

Site 1 was chosen to be within LOS of DSS-13 and with a distance large enough that DSS-13 was in the far field of the emitter antenna. Figure 3 is a photograph of the site, looking at DSS-13. The transmit power was reduced to -5 dBm for this site, because of the short distance. For Site 1, the dependence of received power on offset angle reflects the gain pattern of the emitter antenna. This measured dependence is regarded as the baseline for comparing results obtained from Sites 2 and 3, both without LOS to DSS-13.



Figure 3. View toward DSS-13 from Site 1.

Site 2 is separated from DSS-13 by a small hill, within a few minutes' drive from DSS-13. This site was selected to verify that the signal could be received at DSS-13 despite the lack of an LOS and therefore to verify approximately the trans-horizon propagation loss model used.

Site 3 was selected based on the following criteria. There should be no LOS, and the distance should be significantly larger than for Site 2. When the emitter antenna points along the great circle path toward DSS-13, the received power should be at least 20 dB larger than the minimum detectable power, so that 20 dB of loss due to offset angle can be measured. The site should be isolated from busy traffic but accessible by roadways, satisfying logistical and safety requirements. In the end, Site 3 was selected 32.4 km from DSS-13 near the small community of Harvard. Figure 4 shows the view from this site toward DSS-13.

III. Measurements

At each site, the same basic procedure was followed. The location was accurately determined by means of a GPS receiver. This location and the known location of DSS-13 were employed in calculating the azimuth toward DSS-13. At the other end of the link, the azimuth of DSS-13 was set to that of the emitter site. The elevation angle of DSS-13 was set to 7 deg; this is the lowest elevation angle permitted for DSS-13. The receiving chain for right-hand circular polarization was used for power measurements.



Figure 4. View toward DSS-13 (behind small hill at center of figure) from Site 3.

At Site 1, the transmit power was set to -5 dBm, and an unmodulated carrier employed. The emitter antenna was initially pointed directly at DSS-13 along the LOS. Then the azimuth of the emitter antenna was adjusted in 1-deg steps in both directions, in order to introduce offset angles relative to the direction of maximum received power. At each new azimuth, the received power was measured. Since DSS-13 was in the far field of the 1-m emitter antenna, it was expected that the dependence of received power on offset angle would correspond to the far-field gain pattern of the emitter antenna.

At Sites 2 and 3, where there is no LOS, the azimuth of the emitter antenna was initially set approximately to that of the great circle path toward DSS-13. The elevation angle of the emitter antenna was set to the horizon elevation angle. The transmit power was set to 1 W, and an unmodulated carrier was employed. The azimuth was then adjusted in 1-deg steps on either side of the initial azimuth. The received power was measured at each of these azimuths.

Figure 5 shows the dependence of the received power on offset angle of the emitter antenna. There is a data set for each of the three emitter sites. For each data set, the received power is normalized by a reference power. The purpose of the normalization is to allow the three data sets to appear in Figure 5 with an approximately common maximum value. This facilitates comparisons of the widths of the three data sets.

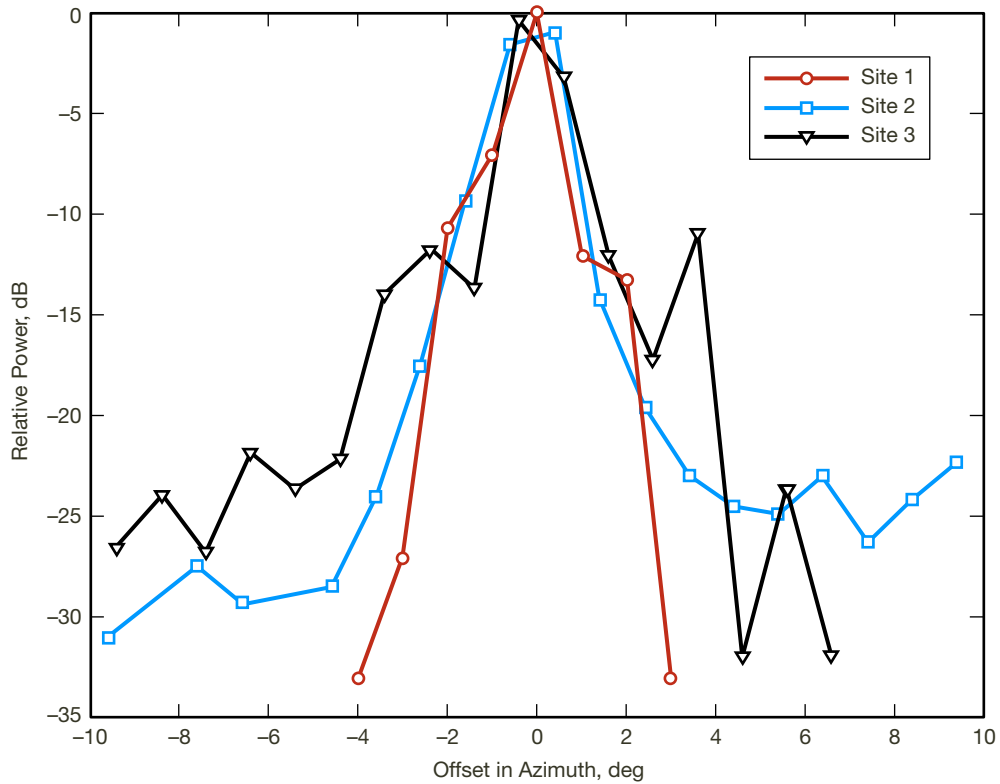


Figure 5. Relative received power plotted against the offset angle for the emitter antenna.

For Site 1, the reference power, -29.9 dBm, equals the received power when the emitter antenna was pointed along the LOS toward DSS-13. The Site 1 data set represents the far-field antenna gain pattern of the emitter antenna.

For Site 2, the reference power, -36.0 dBm, is the estimated power that would have been delivered had the emitter antenna been pointed more precisely in azimuth. The maximum measured power was -37.0 dBm at an azimuth that was estimated to be 0.4 deg off the azimuth of the great circle path toward DSS-13.

For Site 3, the reference power, -73.0 dBm, is the estimated power that would have been delivered had the emitter antenna been pointed more precisely in azimuth. The maximum measured power was -73.4 dBm at an azimuth that was estimated to be 0.4 deg off the azimuth of the great circle path toward DSS-13.

There are limitations in the accuracy of the measured results. First, the horizontal resolution of Figure 5 is no finer than 1 deg, because the emitter antenna controller could only change the azimuth angle in 1 -deg steps. Second, the feed position of the emitter antenna, the only movable element of that antenna, was not optimized during initial calibration at Site 1, for lack of time. Measurements at Site 1 show unexpected variations at offset angles near 1 deg and 2 deg. The measurements were not repeated due to a time limitation at Site 1. These uncertainties need to be resolved in future testing. The feed position, and hence the antenna gain pattern, remained unchanged when the emitter antenna was relocated to Sites 2 and 3.

IV. Analysis of Results

The primary purpose of these tests is to determine how the power delivered to the receiver decreases as the offset angle of the emitter antenna increases. For this purpose, the relative powers shown in Figure 5 are adequate. However, it is also of interest to compare the calculated and the measured absolute power received when the emitter antenna was pointed in the direction corresponding to the maximum delivery of power to DSS-13.

A. Received Power When Emitter Antenna Pointed at DSS-13

For each of the three sites, a link budget appears in Table 2. The link budget represents the case where the emitter antenna is pointed at DSS-13 (for Site 1) or pointed along the great circle path toward DSS-13 with elevation angle equal to the horizon elevation angle (for Sites 2 and 3). Appearing underneath each link budget is the maximum measured power when transmitting from the corresponding site. For Sites 2 and 3, it is believed that the emitter antenna was pointing about 0.4 deg off the desired great circle path when the received power was measured; hence, a somewhat larger received power might have been possible if the pointing of the emitter antenna had been more precise. For all three links, the measured power and calculated power agree to within about 3 dB.

Table 2. Link budgets.

Parameter	Site 1	Site 2	Site 3
Transmit Power	-5 dBm	30 dBm	30 dBm
Transmit Cable Loss	-6 dB	-6 dB	-6 dB
Transmit Antenna Gain	35 dBi	35 dBi	35 dBi
Transmit Pointing Loss	-1 dB	-1 dB	-1 dB
Propagation Loss	-129.3 dB	-175.2 dB	-207.9 dB
Receive Antenna Gain	5.0 dBi	8.8 dBi	8.9 dBi
Received Power at LNA Input	-101.3 dBm	-108.4 dBm	-141.0 dBm
LNA → RID Gain	84.3 dB	84.3 dB	84.3 dB
RID → Spectrum Analyzer Loss	-13.8 dB	-13.8 dB	-13.8 dB
Calculated Power	-30.8 dBm	-37.9 dBm	-70.5 dBm
Measured Power	-29.9 dBm	-37.0 dBm	-73.4 dBm

LNA = low-noise amplifier; RID = RF-to-IF downconverter

The boresight gain of the 1-m emitter antenna at 32 GHz is approximately 35 dBi. This was determined by measuring the received power in a calibration link that employed the 1-m antenna at the receiving end. All link parameters were known in the calibration link except the gain of the 1-m antenna. The calibration was performed at Site 1 before the first test with DSS-13. A horn antenna of known gain transmitted an unmodulated 32-GHz carrier to the 1-m dish. The LOS path was of sufficient length that the horn antenna was in the far field of the 1-m antenna.

The propagation losses were calculated considering the LOS path for Site 1 and the trans-horizon paths for Sites 2 and 3. The mathematical models of Recommendation ITU-R P.452 [2] were employed along with terrain profiles. For the link between Site 3 and DSS-13, the terrain profile is shown in Figure 6. A hill between Site 3 and DSS-13 (and much closer

to DSS-13) determines the horizon for both antennas along the great circle path connecting them.

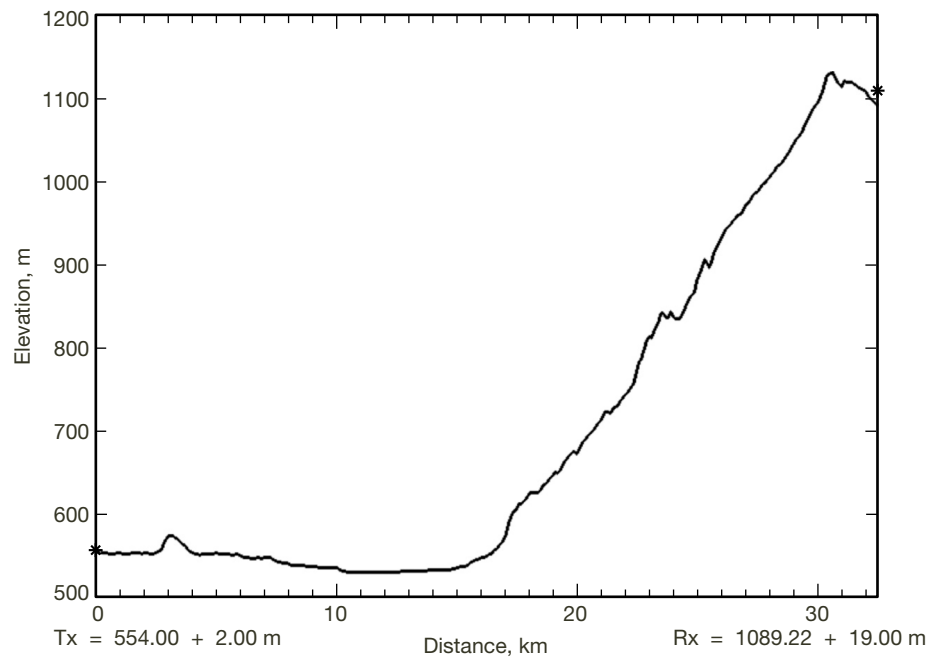


Figure 6. Terrain profile for the path from Site 3 to DSS-13.

The trans-horizon propagation losses for the Site 2 link and the Site 3 link were calculated for the clear-air mode. This mode comprises three propagation mechanisms: diffraction, tropospheric scatter, and anomalous propagation. Diffraction was, in fact, the dominant mode for both of these links, as determined by consideration of the distances and terrain. The parameters used in the propagation loss calculations follow. The frequency was 32 GHz. The emitter antenna height was 2 m. The height of the phase center of the 34-m antenna was taken to be 19 m. The time percentage was 50 percent, representing median meteorological conditions. The refractive index lapse rate over the lowest kilometer of the atmosphere was taken to be 50 N-units/km. The sea-level surface refractivity was taken to be 310 N-units.

For all three links, the DSS-13 elevation angle was set to the lower limit of 7 deg. For the Site 1 LOS link, the emitter was at an elevation angle of -3.1 deg as viewed from DSS-13; therefore, the angle off boresight at DSS-13 was 10.1 deg. For the Sites 2 and 3 trans-horizon links, the elevation angle of the incoming emitter signal would have equaled the horizon elevation angle; for the phase center of the 34-m antenna, the horizon elevation angle was 0 deg and 0.1 deg for the Site 2 link and Site 3 link, respectively. Therefore, the angle off boresight at DSS-13 was 7.0 deg and 6.9 deg for the Site 2 link and Site 3 link, respectively.

The receive antenna gains in Table 2 represent the antenna gain of DSS-13 in the direction of the incoming emitter signal. The emitter, in every case, was in the near field of the 34-m

antenna. However, for angles off boresight of about 7 deg or greater, the near-field and far-field gains [4] are approximately the same, within 1 dB.¹ The far-field envelope gain pattern of Recommendation ITU-R SA.1811 [5] was used to model the 34-m antenna gain. For an angle of 10.1 deg, 7.0 deg, and 6.9 deg, the antenna gain is approximately 5.0 dBi, 8.8 dBi, and 8.9 dBi, respectively.

It was essential to calibrate the gain profile of the DSS-13 RCP receiving chain. This was done by applying an aperture ambient load of 14.7 deg C (287.7 K) to the feed horn. The narrowest bandwidth in the receiving path was 500 MHz, occurring in the RF-to-IF down-converter (RID). The front-end gain, from the feed horn through the low-noise amplifier (LNA) and the RID, was determined by comparing the power spectral density at the RID output to the known power spectral density at the feed horn. The loss in the receiving path between the RID output and the spectrum analyzer input, where received power was measured, was determined by comparing the power in 500 MHz appearing at the spectrum analyzer to that at the output of the RID.

Using the parameter values described above (and appearing in Table 2), it was possible to calculate the power that should have appeared at the spectrum analyzer in the RCP receiving chain. There are, of course, uncertainties in the parameters. Moreover, the accuracies of the trans-horizon propagation loss models are not characterized by the ITU-R. The last two numbers in each column of Table 2 show the calculated and the measured received power.

B. Dependence of Relative Received Power on Offset Angle of Emitter Antenna

The data of Figure 5 indicate clearly that the received power decreases more slowly with increasing offset angle when the link has no LOS (Sites 2 and 3). For example, with an offset angle about 3 deg, the relative received power is larger for Site 2 by about 10 dB and larger for Site 3 by about 18 dB than for the LOS Site 1 link. These data can be explained by the existence of alternate paths, as discussed in Section I and illustrated in Figure 1.

For Site 1, the power is delivered along the LOS path. As the emitter antenna points away from the LOS path, the received power decreases with the transmit antenna gain in the direction of the DSS. Therefore, the data for Site 1 reflect the gain pattern of the emitter antenna.

For Sites 2 and 3 with no LOS to the DSS, the measured data indicate that the dominant path for power delivery is not in the vertical plane containing the great circle path. The dominant path actually changes as the emitter antenna points away from the great circle path. For every offset in azimuth, the dominant path appears to lie in the plane defined by the emitter, the boresight of the emitter antenna and the DSS. This plane changes with the azimuth offset of the emitter antenna. The transmit antenna gain remains approximately constant along the dominant path. However, both the propagation loss and the receive antenna gain vary due to the changing geometry. As the azimuth offset of the emitter

¹ V. Jamnejad, "Near-Field Plots — 34-m / 32 GHz" (internal document), Jet Propulsion Laboratory, Pasadena, California, July 2003.

antenna increases, both the dominant path length and the diffraction angle gradually increase. The variation in receive antenna gain is relatively small because the received power does not arrive along the boresight of the DSS antenna for any azimuth offset of the emitter antenna, not even for zero offset.

When there is no LOS and the interference power arrives off the boresight of the DSS antenna, Figure 5 indicates that the received power decreases more gradually with increasing azimuth offset of the emitter antenna than for the LOS case. In other words, a larger offset angle will be needed in the trans-horizon case to effect the same reduction as in the LOS case. This experimentally observed fact should be taken into account both when aggregate EIRP is calculated and when a mitigation study is undertaken.

Similar measurements to those described above should be conducted at other DSSs and for a larger set of azimuths in order to fully characterize the site shielding of a DSS by surrounding hills. It should be borne in mind that at some DSSs the terrain in some directions may provide less protection than the hills surrounding DSS-13 when looking in the directions of Site 2 and Site 3.

V. Conclusions

In anticipation of potential HDFS deployments, a set of terrestrial interference tests was done at DSS-13. An example emitter was first placed within LOS of DSS-13 at a distance of 2.1 km, and later the emitter was moved to sites that were 3.8 and 32.4 km distant from DSS-13, without LOS. From each of the three sites, an unmodulated 32-GHz carrier was transmitted in the general direction of DSS-13, and the received power was measured. When the emitter antenna pointed at DSS-13 (along the great circle path toward DSS-13 for the trans-horizon sites), the measured power agreed with the calculated power to within about 3 dB. Although the sample size was small, this result nevertheless provided a validation of the ITU-R propagation loss models used in the link calculation. When the emitter antenna pointed away from DSS-13, the received power decreased quickly with increasing offset angle for the LOS case, according to the gain pattern of the emitter antenna, and decreased much more slowly for the trans-horizon cases. In other words, in a trans-horizon case the emitter antenna must be pointed away from the azimuth of the great circle path toward the DSS by a larger angle to effect the same reduction. This observed fact should be taken into account both when aggregate EIRP is calculated and when a mitigation study is undertaken.

Acknowledgments

The authors thank Paul Dandrenos for operation of DSS-13 and assistance in conducting measurements, Arthur Freiley for measuring the gain profile of the DSS-13 receiving chain, Vahraz Jamnejad for characterizing the far-field and near-field gain of 34-m antennas, and Selahattin Kayalar and Charles Wang for review of this manuscript.

References

- [1] T. Peng, P. Kinman, S. Kayalar, and C. Ho, "Estimating the Aggregate Interference from High-Density Fixed Service Emitters to Deep-Space Earth Stations," *The Interplanetary Network Progress Report*, vol. 42-179, Jet Propulsion Laboratory, Pasadena, California, pp. 1–27, November 15, 2009.
http://ipnpr.jpl.nasa.gov/progress_report/42-179/179B.pdf
- [2] International Telecommunication Union, "Prediction Procedure for the Evaluation of Microwave Interference Between Stations on the Surface of the Earth at Frequencies Above About 0.7 GHz," Recommendation ITU-R P.452.
- [3] C. Ho, K. Angkasa, P. Kinman, and T. Peng, "Propagation Loss for Trans-Horizon Interferences in the Regions Surrounding Deep Space Network Complexes," *The Interplanetary Network Progress Report*, vol. 42-162, Jet Propulsion Laboratory, Pasadena, California, pp. 1–20, August 15, 2005.
http://ipnpr.jpl.nasa.gov/progress_report/42-162/162J.pdf
- [4] V. Jamnejad, "A Study of Near to Far Fields of JPL Deep Space Network (DSN) Antennas for RFI Analysis," IEEE Aerospace Conference, Big Sky, Montana, March 6–13, 2004.
- [5] International Telecommunication Union, "Reference Antenna Patterns of Large-Aperture Space Research Service Earth Stations to be Used for Compatibility Analyses Involving a Large Number of Distributed Interference Entries in the Bands 31.8–32.3 GHz and 37.0–38.0 GHz," Recommendation ITU-R SA.1811, 2007.